Transmission of Solitary Pulse in Dissipative Nonlinear Transmission Lines

E. Kengne[1, 2,*] and R. Vaillancourt[1]
[1]*Department of Mathematics and Statistic, University of Ottawa. 585 King Edward Avenue, Ottawa, ON, K1N 6N5, Canada*
[2]*Department of Mathematics & Computer Science, Faculty of Science, University of Dschang. P.O. Box 4509, Douala, Republic of Cameroon*

(Dated: August 28, 2008)

A class of dissipative complex Ginzburg–Landau (DCGL) equations that govern the wave propagation in dissipative nonlinear transmission lines is solved exactly by means of the Hirota bilinear method. Two-soliton solutions of the DCGL equations, from which the one-soliton solutions are deduced, are obtained in analytical form. The modified Hirota method imposes some restrictions on the coefficients equations, namely, the second-order dispersion must be real. The physical requirement of the solutions imposes complementary conditions on the combination of the dispersion and nonlinear gain/loss terms of the equation, as well as on the coefficient of the Kerr nonlinearity. The analytical solutions for one-solitary pulses are tested in direct simulations.

On empoie la méthode biliéaire d'Hirota pour trouver la solution exacte d'une classe d'équations de Ginzburg–Landau complexes et dissipatives qui gouvernent la propagation d'ondes dans une ligne de transmission non-linéaire dissipative. On obtient analytiquement les solutions à deux solitons de ces équations d'où l'on tire les solutions à un soliton. La méthode d'Hirota modidfiée impose des restrictions sur les coefficients des équations, en particulier, la dispersion du second ordre doit être réelle. La dimension physique des solutions impose des conditions complémentaires sur la combinaison des termes de gain/perte de l'équation ainsi que sur le coefficient de la non-linéarité de Kerr. On teste les solutions analytiques des impulsions solitaires en simulations directes.

PACS numbers: 03.75.Gg, 03.75.Nt, 03.75.Hh, 02.60.Cb

To appear in *Communications in Nonlinear Science and Numerical Simulations*

I. INTRODUCTION

Since the 1970s, various investigators have discovered the existence of solitons in nonlinear transmission lines (NLTLs), through both mathematical models and physical experiments (see for example Refs. [1–5]). Scott's classical monograph [6] was among the first to treat the physics of transmission lines. Scott showed that the Korteweg–deVries (KdV) equation describes weakly nonlinear waves in a nonlinear LC transmission line containing a finite number of cells which consist of two elements: a linear inductor in the series branch and a nonlinear capacitor in the shunt branch. If the nonlinearity is moved from the capacitor parallel to the shunt branch of the line to a capacitor parallel to the series branch, the nonlinear Schrödinger (NLS) equation is obtained instead [7].

Some years ago, the nonlinear propagation of signals in electrical transmission lines has been investigated, theoretically and experimentally [5, 8, 9]. It has been shown that the system of equations governing the physics of the considered network can be reduced either to single or coupled NLS equations or to the Ginzburg-Landau (GL) equations. The single and the coupled NLS equations admit the formation of envelope solitons, which have been observed experimentally [8, 9].

More recently, Pelap et al. [10] presented a model for wave propagation on a discrete dissipative electrical transmission line of Fig. 1 based on the complex Ginzburg–Landau (CGL) equation

$$i\frac{\partial A}{\partial t} + P\frac{\partial^2 A}{\partial x^2} + Q\left|A\right|^2 A = i\gamma A, \tag{1}$$

derived in the small amplitude and long wavelength limit using the standard reductive perturbation technique and complex expansion [11] of the governing nonlinear equations. Here A is a complex amplitude, $P = P_r + iP_i$ and

*Corresponding author's E-mail: ekengne6@yahoo.fr

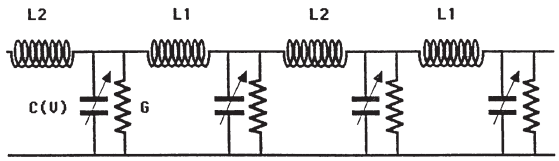

FIG. 1: Representation of a discrete nonlinear dissipative bi-inductance transmission line.

$Q = Q_r + iQ_i$ are two complex constants, and γ is a positive constant. Basically, the evolution of the complex wave envelope A is controlled by the competition of the dispersion $(\sim P)$, nonlinearity $(\sim Q)$, and linear gain γ. Physically, P_r measures the wave dispersion, P_i measures the relative growth rate of disturbances whose spectra are concentrated near the fundamental wavenumber k, Q_r determines how the wave frequency is amplitude modulated, Q_i measures the saturation of the unstable wave, and the positive constant γ is the linear gain. The modulational instability of the Stokes waves $A(x,t) = A_0 \exp\left[ik_0 x - i\left(P_r k_0^2 - Q_r |A_0|^2\right)t\right]$, where $Q_i |A_0|^2 = \gamma + P_i k_0^2$, is considered in Ref. [10] and the modulational instability criterion $P_r Q_r + P_i Q_i > 0$ has been found.

In this work, we study the transmission of solitary pulses, governed by the GL equation (1), propagating in the network of Fig. 1. The paper is structured as follows. In section 2, we show how the modified Hirota method is applied to construct the exact solitary pulse solutions of the DCGL equation. In section 3, we present some numerical results, and the paper is concluded in section 4.

II. DERIVATION OF EXPLICIT SOLITARY PULSE SOLUTIONS

In order to prove that Eq. (1) can support envelope solitons, we use the Hirota bilinear technique [12]. Thus, we follow the definition of Nozaki and Bekki [13, 14] and introduce the modified Hirota derivative

$$D_{\alpha,t}^m D_{\alpha,x}^n F.G = \left(\frac{\partial}{\partial t'} - \alpha\frac{\partial}{\partial t}\right)^m \left(\frac{\partial}{\partial x'} - \alpha\frac{\partial}{\partial x}\right)^n F(x,t)\, G(x',t')\Big|_{x'=x,t'=t}. \tag{2}$$

We first note that Eq. (1), under the transformation $A(x,t) = \psi(x,t)\exp(\gamma t)$, takes the form

$$i\psi_t + P\psi_{xx} + Q\exp(2\gamma t)|\psi|^2\psi = 0. \tag{3}$$

The two-soliton solution of Eq. (3) is given by

$$\psi(x,t) = u_1(x,t) + u_2(x,t), \tag{4}$$

where $u_1(x,t)\, u_2(x,t) = 0$ corresponds to the single soliton. Inserting Eq. (4) into Eq. (3), we obtain the system

$$\begin{aligned} &i\frac{\partial u_1}{\partial t} + P\frac{\partial^2 u_1}{\partial x^2} + Q\exp(2\gamma t)|u_1|^2 u_1 + Q\exp(2\gamma t)\left(2|u_1|^2 u_2 + u_1^2 u_2^*\right) = 0, \\ &i\frac{\partial u_2}{\partial t} + P\frac{\partial^2 u_2}{\partial x^2} + Q\exp(2\gamma t)|u_2|^2 u_2 + Q\exp(2\gamma t)\left(2|u_2|^2 u_1 + u_2^2 u_1^*\right) = 0, \end{aligned} \tag{5}$$

where "*" stands for the complex conjugate. To obtain exact solutions of system (5) we adopt the modified Hirota ansatz

$$u_1(x,t) = G(x,t)\, F^{-\alpha}(x,t), \quad u_2(x,t) = H(x,t)\, F^{-\alpha}(x,t), \tag{6}$$

where G and H are two complex functions, F is a real function, and α is, in general, complex. Due to the presence of power $-\alpha$, transformation (6) is different from that used in the case of the conventional nonlinear Schrödinger system. This difference is, as a matter of fact, the main motivation for introducing these modified Hirota derivatives. Expression (6) is deduced from the truncation of the Puiseux expansions at the lowest level [15]. Using Eq. (6), Eq. (5) is rewritten as a pair of bilinear equations in terms of the modified Hirota derivative (2),

$$\left[iD_{\alpha,t} + PD_{\alpha,x}^2 + iP\beta + 2ix\beta PD_{\alpha,x}\right]F.G = 0, \quad \left[iD_{\alpha,t} + PD_{\alpha,x}^2 + iP\beta + 2ix\beta PD_{\alpha,x}\right]F.H = 0, \tag{7}$$

$$D_x^2 F.F = \frac{2Q\exp(2\gamma t)\left(2HG^* + GH^* + GG^*\right)}{P\alpha(1+\alpha)F^{2\mathrm{Re}\alpha-2}}, \quad D_x^2 F.F = \frac{2Q\exp(2\gamma t)\left(2GH^* + HG^* + HH^*\right)}{P\alpha(1+\alpha)F^{2\mathrm{Re}\alpha-2}}, \tag{8}$$

for $GH \neq 0$. So the left-hand sides of Eq.(8) become equal. Hence the right-hand sides of Eq. (8) should also be equal which is true only under the bilinear condition

$$(H+G)\left(G^{*}-H^{*}\right)=0, \tag{9}$$

that is, $H=\varepsilon G$ with $\varepsilon=\pm 1$. In what follows, we consider that $\varepsilon \in\{-1,\ 0,\ 1\}$, $\varepsilon=0$ corresponding to the single soliton propagating in the network. We then obtain

$$\left[iD_{\alpha,t}+PD_{\alpha,x}^{2}\right]F.G=0, \tag{10}$$

$$D_{x}^{2}F.F=\frac{2Q\exp\left(2\gamma t\right)\left(1+3\varepsilon\right)}{P\alpha\left(1+\alpha\right)F^{2\mathrm{Re}\alpha-2}}GG^{*}. \tag{11}$$

For the special case $\alpha=1+i\eta$, with real η, (10)–(11) is a system with time-dependent coefficients. For simplicity, we will restrict ourselves to this special case. Having obtained the bilinear condition and bilinear forms, our next aim is to obtain the soliton solutions. To generate the soliton solutions, we assume an expansion of the form

$$G=\exp\left(xh_{1}\left(t\right)+h_{0}\left(t\right)\right),\quad F=1+N\left(t\right)\exp\left[x\left(h_{1}\left(t\right)+h_{1}^{*}\left(t\right)\right)+h_{0}\left(t\right)+h_{0}^{*}\left(t\right)\right]. \tag{12}$$

Instead of taking h_0 and h_1 constant as in the conventional nonlinear Schrödinger system, we take h_0 and h_1 to be functions of time t, because we want to solve a system with time-varying coefficients, or, in other words, for the waves propagating in an inhomogeneous medium. Inserting Eq. (12) into system (10)–(11), we obtain

$$h_{1}'=0,\quad h_{0}'-iPh_{1}^{2}=0,\quad \frac{N'}{N}=P\eta\left(h_{1}+h_{1}^{*}\right)^{2}, \tag{13}$$

$$Q\left(1+3\epsilon\right)\exp\left(2\gamma t\right)=\frac{\alpha\left(1+\alpha\right)}{2}PN\left(h_{1}+h_{1}^{*}\right)^{2}. \tag{14}$$

From Eq. (13) we obtain

$$h_{1}\left(t\right)=k_{1},\quad h_{0}\left(t\right)=iPk_{1}^{2}t+\xi_{0},\quad N\left(t\right)=N_{0}\exp\left[P\eta\left(k_{1}+k_{1}^{*}\right)^{2}t\right], \tag{15}$$

where k_1 and ξ_0 are two complex constants and N_0 a real constant. If N_0, η, and $N(t)$ are real, the definition of $N(t)$ in Eq. (15) requires P to be real. If $N(t)$ and P are reals, but $\alpha=1+i\eta$ complex, Eq. (11) requires Q to the complex too. Working with real P means that we do not include diffusion, which would be represented by an imaginary part of P [16–19]. However, the nonlinear coefficient Q which is complex allows the combination of the self-phase-modulation with the nonlinear loss/gain. Thus, the diffusion term P and the nonlinear gain/loss Q term are necessary ingredients for the applicability of the method. Form condition (14) we obtain

$$\left(k_{1}+k_{1}^{*}\right)^{2}=\frac{4\gamma Q_{i}}{P\left(-3Q_{r}\pm\sqrt{9Q_{r}^{2}+8Q_{i}^{2}}\right)},\quad N_{0}=\frac{\left(1+3\epsilon\right)Q_{i}}{3\gamma},\quad \eta=\frac{-3Q_{r}\pm\sqrt{9Q_{r}^{2}+8Q_{i}^{2}}}{2Q_{i}}. \tag{16}$$

As it is seen from Eq. (16), the coefficient η, which determines the chirp of the pulse, depends only on the nonlinear gain/loss term. Because $P=P_r$ is real and $\gamma>0$, the physical solutions are those that make $\left(k_1+k_1^*\right)^2$ positive, that is, as one can see from Eq. (16), $P=P_r$ and $Q=Q_r+iQ_i$ must satisfy the condition

$$Q_{i}P_{r}\left(-3Q_{r}\pm\sqrt{9Q_{r}^{2}+8Q_{i}^{2}}\right)>0. \tag{17}$$

Because of the transformation $A\left(x,t\right)=\psi\left(x,t\right)\exp\left(\gamma t\right)$, we obtain from Eq. (4) that

$$A\left(x,t\right)=u_{1}\left(x,t\right)\exp\left(\gamma t\right)+u_{2}\left(x,t\right)\exp\left(\gamma t\right)=A_{1}\left(x,t\right)+A_{2}\left(x,t\right).$$

From Eqs. (6), (12), (15), and (17), we obtain the following soliton

$$\begin{aligned}A_{1}\left(x,t\right)&=\frac{\exp\left[k_{1}x+\left(iPk_{1}^{2}+\gamma\right)t+\xi_{0}\right]}{\left(1+N_{0}\exp\left[\left(k_{1}+k_{1}^{*}\right)x+P\left\{\eta\left(k_{1}+k_{1}^{*}\right)^{2}+i\left(k_{1}^{2}-k_{1}^{*2}\right)\right\}t+\xi_{0}+\xi_{0}^{*}\right]\right)^{1+i\eta}},\\ A_{2}\left(x,t\right)&=\varepsilon A_{1}\left(x,t\right),\qquad \varepsilon\in\{-1,\ 0,\ 1\},\end{aligned} \tag{18}$$

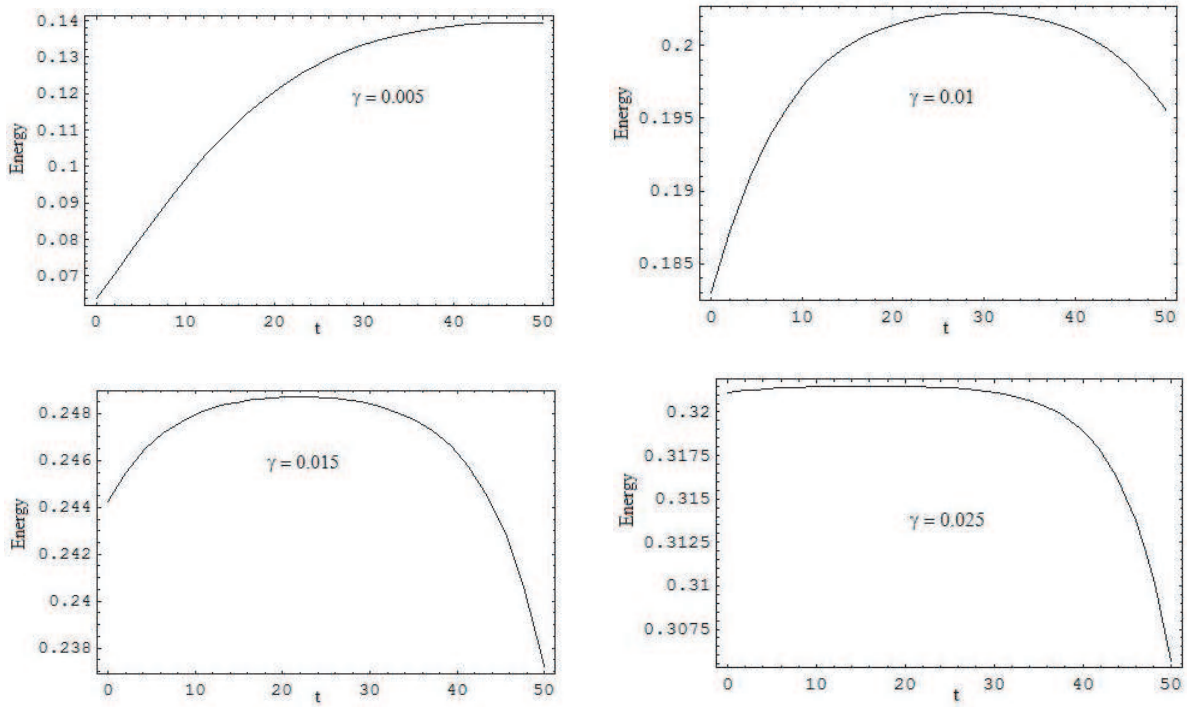

FIG. 2: Evolution of the energy of the one-solitary pulse versus time t for the parameter values $P = 0.5$, $Q = -0.25 + i$, $k_{1i} = 1$, $\xi_0 = 0.1 + i$, and for different values of the linear gain γ. Here, we have used $k_{1r} > 0$ and $\eta > 0$.

where k_1, N_0, and η satisfy condition (16). Solution (18) contains two free parameters, namely, the complex parameter ξ_0 and the real constant $k_{1i} = \text{Im } k_1$. It follows from Eq. (18) that the physical solutions are those that correspond to positive N_0. As one can see from Eq. (16), the physical solution then corresponds to positive Q_i for $\varepsilon \in \{0,\ 1\}$ and $Q_i < 0$ for $\varepsilon = -1$ (we remember that $\gamma > 0$). By setting $k_1 = k_{1r} + ik_{1i}$ and $\xi_0 = \xi_{0r} + i\xi_{0i}$, it is seen from Eqs. (16) and (18) that the amplitude of the solitary pulse is given by

$$|A_1(x,t)| = |A_1(z = x - vt)| = \frac{\exp(\xi_{0r})}{N_0 \exp(2\xi_{0r}) \exp(k_{1r}z) + \exp(-k_{1r}z)}, \quad v = \frac{2Pk_{1i}k_{1r} - \gamma}{k_{1r}}, \tag{19}$$

and this means that the solitary pulse moves with velocity $v = \frac{2Pk_{1i}k_{1r} - \gamma}{k_{1r}}$, which is an arbitrary constant. The wavenumber is then k_{1r}. If we take $\xi_{0r} = -\ln\sqrt{N_0}$, Eq. (19) coincides with the moving soliton $|A_1(z)| = 1/\left(2\sqrt{N_0}\cosh k_{1r}z\right)$. It is seen from Eq. (19) that the soliton amplitude increases with ξ_{0r}.

Note: According to Eq. (4), the one-soliton solutions of Eq. (1) are obtained for Eq. (15) as follows: If $\varepsilon = 0$, then $A(x,t) = A_1(x,t)$; if $\varepsilon = 1$, then $A(x,t) = 2A_1(x,t)$. These two solutions are distinct, not only because of the factor 2, but also because of the expression for N_0 appearing in the expression of $A_1(x,t)$ (see Eq. (18)). We note that for $\varepsilon = -1$, we obtain from Eq. (4) the zero solution of Eq. (1).

As one can see from Eq. (19), the energy of the one-soliton will depend on the linear gain γ. For different values of the linear gain γ, we plot in Figure 2 the soliton's energy versus time t with the parameter values $P = 0.5$, $Q = -0.25 + i$, $k_{1i} = 1$, and $\xi_0 = 0.1 + i$. It follows from the plots of Figure 2 that the soliton's energy increases with the linear gain and the form of its curve as function of time t depends on the value of the linear gain γ : some values of γ correspond to a monotonic growth/decay of energy, while some other values of γ correspond to a non monotonic growth/decay of energy.

Note that a solitary pulse is of interest if it is stable, a necessary condition for this is the stability of the zero background, i.e., the trivial solution $A(x,t) = 0$. As it has been shown in work [10], the necessary condition for the stability of the zero background is that $P_rQ_r < 0$ (we remember that the solitary pulse solution obtained in the present work are valid only for $P_i = 0$).

From a detailed investigation, we find that Eq. (1) admits the higher order one-solitary pulse solutions which can be constructed using the Hirota bilinear method for the conditions

$$P_i = 0,\ Q_i > 0,\ P_r\left(-3Q_r \pm \sqrt{9Q_r^2 + 8Q_i^2}\ \right) > 0. \tag{20}$$

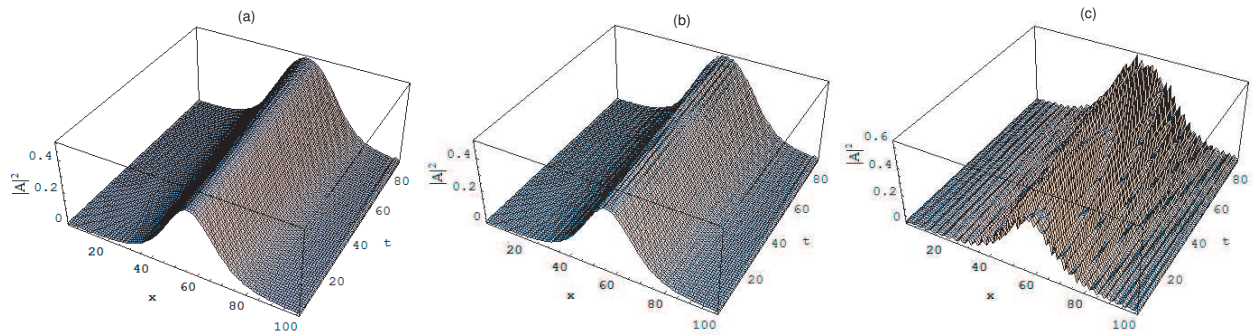

FIG. 3: Propagation of the solitary pulse for $P = -0.5$, $Q = 0.25 + 0.05i$, $\gamma = 0.025$, $\xi_0 = 0.1 + i$, $k_{1i} = 1$, $\eta < 0$, and $k_{1r} > 0$. The relative amplitude of the initial perturbation is 0.1% in (a), 0.5% in (b), and 3.75% in (c).

The necessary condition for the stability of these solitary pulse solutions is

$$P_r Q_r < 0. \tag{21}$$

III. STABILITY OF SOLITARY PULSES

In this section, we want to test by numerical simulations the stability of exact one-solitary pulse solutions generated by the above modified Hirota method. We used the Crank–Nicholson form of the discrete representation of Eq. (1), as it is stable and accurate to second order in space and time [20]. To demonstrate the stability of the solitary pulses, we add random perturbations to the initial profile, whose unperturbed shape corresponds to the exact solution of Eq. (1). Actually, a relatively weak random noise (at the δ % amplitude level) was added, and as the exact solution of Eq. (1), we have used the one-soliton solution that corresponds to $\varepsilon = 0$ (see Eq. (18) and the note after Eq. (19)), that is,

$$A(x,t) = \frac{\exp\left[k_1 x + \left(iPk_1^2 + \gamma\right)t + \xi_0\right]}{\left(1 + N_0 \exp\left[\left(k_1 + k_1^*\right)x + P\left\{\eta\left(k_1 + k_1^*\right)^2 + i\left(k_1^2 - k_1^{*2}\right)\right\}t + \xi_0 + \xi_0^*\right]\right)^{1+i\eta}}. \tag{22}$$

Zero boundary conditions (ZBC) are used and we simply need to set the values of boundary points to zero. In fact, simulations where the ZBC are used need minimal computational time. Physically, they represent the situation where we have metallic boundaries with infinite conductive properties at each end of the computational window.

A caveat should be made concerning the far-field (background) instability. For sufficiently small A, the evolution of amplitude A is mainly governed by the linear gain γ in Eq. (1), which makes the zero background unstable. Nevertheless, this instability may not manifest itself if γ is reasonably small, and the integration time is not extremely large [21, 22]. The latter circumstance helps make formally unstable solitary pulses stable and physically relevant objects [23]. In fact, the instability of a solution does not exclude its observation in experiments. If the time scale over which the onset of instability occurs far exceeds the duration of the experiments, then the formally unstable solution is as relevant for the experiment as is the stable solution.

In what follows, we describe some sets of simulations which characterize the stability of the solitary pulses. These simulations also show how the equation parameters affect the solitary pulses. For all the simulations, we take P and Q such that the necessary condition of the stability of the solitary pulses (21) is satisfied.

Remark. Because of the presence of the linear gain γ, it is evident that the amplitude of the solitary pulses will increase as the wave propagates.

A. Effect of the random perturbations

Now, we add random perturbations to the initial profile of the solitary pulses, whose unperturbed shape corresponds to the exact solution (22) of Eq. (1). Relatively small random noise at 0.1% and 0.5% amplitude level were added in the case presented in Figs. 3(a) and 3(b), while a random noise at 3.75% amplitude level was added in the case presented in Fig. 3(c). As we can see from these figures, the evolution of the pulse is affected with strong noises (compare for example the maximal amplitudes of the solitary wave on Figs. 3(a), 3(a), and 3(c)).

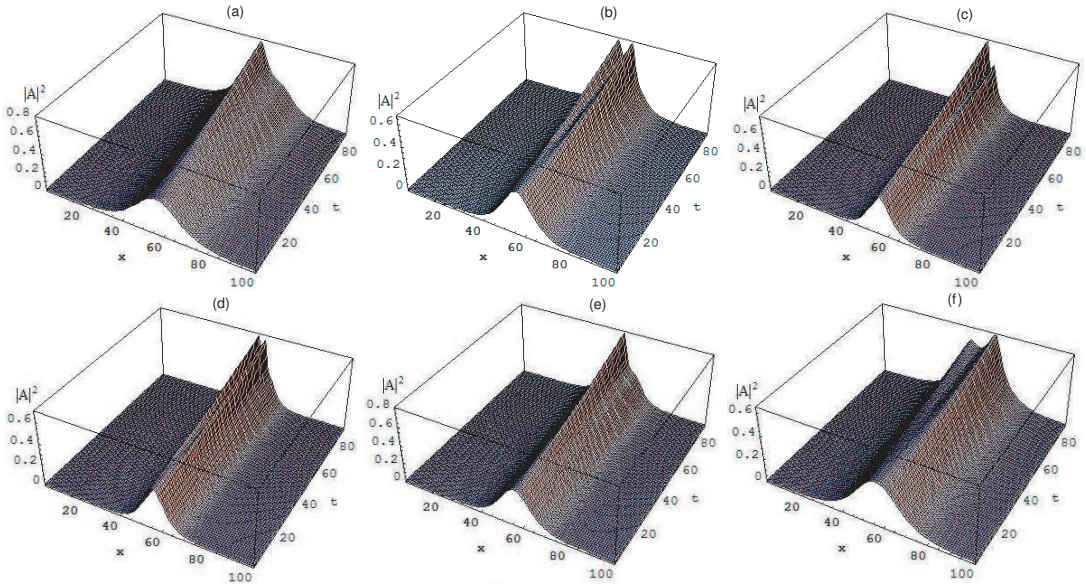

FIG. 4: Propagation of the solitary pulse for different values of the dispersion coefficient P for $Q_i = 0.05$, $\gamma = 0.025$, $k_r > 0$, $k_{1i} = 1$, and $\xi_0 = 0.1 + i$. We have used $\eta > 0$ and $q_r = 1.2$ for positive P, and $\eta < 0$ and $Q_r = -1.2$ for negative P. The relative amplitude of the initial perturbation is 0.1%. The values of $P = -0.1$, $P = -0.05$, $P = -0.025$, $P = 0.025$, $P = 0.05$, and $P = 0.1$ are used for Figs. 4(a), 4(b), 4(c), 4(d), 4(e), and 4(f), respectively.

B. Effect of the dispersion P

To observe the effect of the dispersion on the evolution of the solitary pulses, we consider six values of P, three negative values and three positive values. For all the plots of Fig. 4, we consider the same values of $Q_i = 0.05$, $\xi_0 = 0.1 + i$, and $\gamma = 0.025$. Because we need condition (21) to be satisfied, we will use different values of Q_r : $Q_r = 0.25$ for negative P and $Q_r = -1.2$ for positive P. Figs. 4(a), 4(b), 4(c), (d), (e), and 4(f) correspond to $P = -0.1$, $P = -0.05$, $P = -0.025$, $P = 0.025$, $P = 0.05$, $P = 0.1$. For all the plots of this figure, the relative amplitude of the initial perturbation 0.1% was added. The plots of Fig. 4 show that the width of the soliton increases with $|P|$ and the amplitude of the solitary pulse depend on P, but, is not monotone as function of P. The soliton sharpness is also affected by the dispersion coefficient P. One should note that two P with opposite sign do not correspond to the same evolution of the solitary pulse (this can be well observed from Figs. 4(b) and 4(e)).

C. Effect of the nonlinear gain

Here we present three plots to display the evolution of general wave packets for different values of nonlinear gain. Random noise (0.1%) is used. For all the plots of Figure 5, we have used $P = -0.025$, $Q_r = 2.2$, $\xi_0 = -2 + 0.5i$, $k_{1i} = -1$, $\gamma = 0.025$, $k_{1r} > 0$ and $\eta < 0$. The plot of Figs. 5(a), 5(b), and 5(c) correspond to $Q_i = 0.05$, $Q_i = 0.5$, and $Q_i = 1.5$, respectively (we remember that the one-solitary pulse has been obtained only for positive Q_i (see Eq. (20)). As the plots of Figure 5 show, the width and the amplitude of the wave packets decrease as the nonlinear gain increases.

D. Effect of the linear gain

As we have mentioned above, for sufficiently small A, the evolution of amplitude A is mainly governed by the linear gain γ in Eq.(1), which makes the zero background unstable, and this instability may not manifest itself if γ is reasonably small, and the integration time is not extremely large. In Figure 6, we plot the evolution of the solitary pulses for different values of the linear gain γ when all the other parameters are maintained constant. Thus, we use for Figure 6 the parameter values $P = 0.5$, $Q = -2.2 + 2.5i$, $k_{1i} = -1$, $\xi_0 = -2 - 0.5i$, $\eta > 0$, $k_{1r} < 0$. The relative amplitude of the initial perturbation is 0.1%. Plot (a) gives the propagation of the solitary pulse for the linear gain $\gamma = 0.003$, while plots (b) and (c) correspond to $\gamma = 0.03$ and $\gamma = 0.3$, respectively. For all the plots of Figure 6,

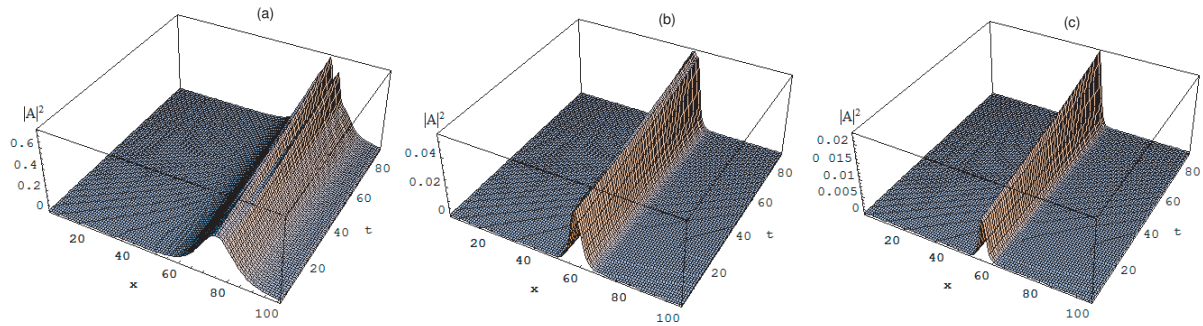

FIG. 5: Propagation of a general wave packet for different values of the nonlinear gain for $P = -0.025$, $Q_r = 2.2$, $\xi_0 = -2+0.5i$, $k_{1i} = -1$, $\gamma = 0.025$, $k_{1r} > 0$ and $\eta < 0$. Plots (a), (b), and (c) correspond to $Q_i = 0.05$, $Q_i = 0.5$, and $Q_i = 1.5$, respectively.

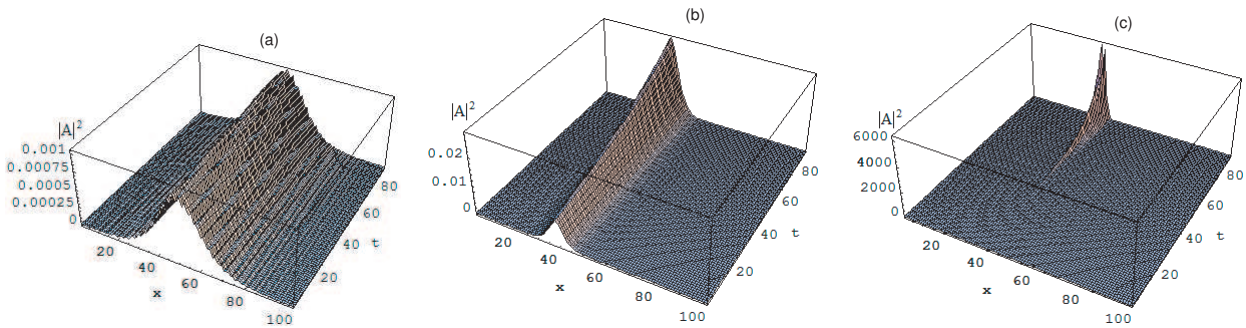

FIG. 6: Plot of the propagation of the solitary pulse for the parameters $P = 0.5$, $Q = -2.2 + 2.5i$, $k_{1i} = -1$, $\xi_0 = -2 - 0.5i$, $\eta > 0$, $k_{1r} < 0$, with relative amplitude of the initial perturbation 0.1%. Plots (a), (b), and (c) show the propagation of the solitary pulse for the linear gain $\gamma = 0.003$, $\gamma = 0.03$, and $\gamma = 0.3$, respectively.

the integration time is taken to be $t = 20$. The plots of this figure show that if the linear gain γ is small, but not extremely small, instability manifests itself.

E. Effect of the solution parameter k_{1i} on the solitary pulse

The three plots of Figure 7 show the evolution of the density of the solitary pulses for different values of the parameter k_{1i}. The solitary pulse we have used for these plots corresponds to the parameters $P = 0.5$, $Q = -0.25 + i$, $\gamma = 0.03$, $\xi_0 = -2 - 0.5i$, $k_{1r} < 0$, and $\eta > 0$. Plots (a), (b) and (c) correspond to $k_{1i} = -1$, $k_{1i} = 0$, and $k_{1i} = 2$ respectively. As these plots show, the energy of the solitary pulse, as well as its curve as function of time t depends on k_{1i}.

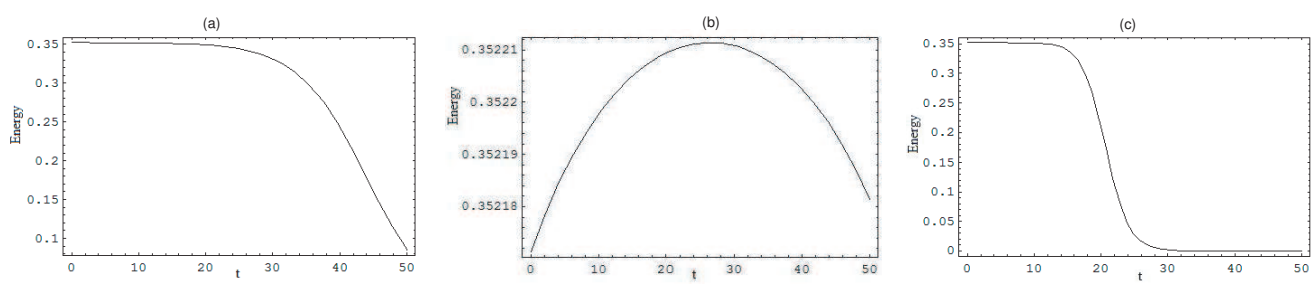

FIG. 7: Evolution of the energy of the solitary pulse for different values of k_{1i} for $P = 0.5$, $Q = -0.25 + i$, $\gamma = 0.03$, $\xi_0 = -2 - 0.5i$, $k_{1r} < 0$, and $\eta > 0$. (a) for $k_{1i} = -1$, (b) for $k_{1i} = 0$, and (c) for $k_{ki} = 2$.

IV. CONCLUSION

By means of the Hirota bilinear method, we have obtained exact solitary pulse solutions for a class of DCGL equation governing wave propagation in dissipative nonlinear transmission lines. To obtain dissipative-soliton solutions to the equation, a modified definition of the Hirota derivative is used. We have first obtained a two-soliton in exact analytical form, and then deduce the one-soliton solution. If the two-soliton solutions can exist for both nonlinear gain ($Q_i > 0$) and nonlinear loss ($Q_i < 0$), it is found that the one-soliton solution correspond only to the nonlinear gain. Direct simulations of the underlying DCGL equations have demonstrated the stability of solitary pulses under the simultaneous action of the linear and nonlinear gain. This does not remain true if a strong random initial perturbation is added. To avoid the blowup of the background within the propagation distance, the linear gain must be reasonably small.

The most essential necessary restriction for the applicability of the modified Hirota method is that the coefficient in front of the dispersive term of the equation must be real, which, in terms of optical physics, implies the absence of spectral filtering, which is the case in many experimentally relevant settings.

---

[1] T.C. Kofane, B. Michaux, and M. Remoissenet, J. Phys. C: Solid State Phys. **21**, 1395 (1988).
[2] P. Marquié, J.M. Bilbault, and M. Remoissenet, Phys. Rev. E **51**, 6127 (1995).
[3] H. Nagashima and H. Amagishi, J. Phys. Soc. Japan **47**, 2021 (1979).
[4] M.S. Ody, A.K. Common, and M.Y. Sobhy, Eur. J. Appl. Math. **10**, 265 (1999).
[5] E. Kengne, B.A. Malomed, S.T. Chui, and W.M. Liu, J. Math. Phys. **48**, 013508 (2007).
[6] A.C. Scott, Active and Nonlinear Wave Propagation in Electronics (Wiley, NewYork, 1970).
[7] V. Nejoh, J. Phys. A **20**, 1733 (1987).
[8] P. Marquié, J. M. Bilbault, and M. Remoissenet, Phys. Rev. E **49**,828 (1994).
[9] J.M. Bilbault, P. Marquié, and B. Michaux, Phys. Rev. E **51**, 817 (1995).
[10] F.B. Pelap, T.C. Kofané, N. Flytzanis, and M. Remoissenet, J. Phys. Soc. Jpn **70**, 2568 (2001).
[11] T. Tanuiti and N. Yajima, J. Math. Phys. **10**, 1369 (1969).
[12] R. Hirota, 1980, Direct method in soliton theory. *Solitons (Topics in Current Physics vol 17)* ed R.K. Bullough and P.J. Candrey (Berlin: Springer) p. 157.
[13] K. Nozaki and N. Bekki, J. Phys. Soc. Jpn. **53** 1581 (1984).
[14] N. Bekki and K. Nozaki, Phys. Lett. A **110** 133 (1985).
[15] E. Yomba and T.C. Kofané, J. Phys. Soc. Jpn **69**, 1027 (2000).
[16] B.A. Malomed, Physica D **27**, 113 (1987); B.A. Malomed and L.C. Nepomnyashchy, Phys. Rev. A **42**, 6009 (1990).
[17] P. Marcq, H. Chate, and R. Conte, Physica D 73 305 (1994); E.N. Tsoy, A. Ankiewicz, and N. Akhmediev, Phys. Rev. E **73**, 036621 (2006).
[18] B.A. Malomed, I.M. Uzunov, M. Golles, and F. Lederer, Phys. Rev. E **55**, 3777 (1997).
[19] I.M. Uzunov, R. Muschall, M. Golles, F. Lederer, and S. Wabnitz, Opt. Commun. **118**, 577 (1995).
[20] W.H. Press, B.P. Flannery, S.A. Teukolsky, and W.T. Vallerling, *Numerical Recipes in Fortran* (Cambridge: Cambridge University Press), 1992.
[21] M.F.S. Ferreira, M.M.V. Facao, and S.C.V. Latas, Fiber Integrated Opt. **19**, 31 (2000).
[22] D.Y. Tang, W.S. Man, H.Y. Tam, and P.D. Drummond, Phys. Rev. A **64**, 033814 (2001).
[23] B.A. Malomed, M.Golles, I.M. Uzunov, and F. Lederer, Phys. Scr. 55, **73** (1997).